Nanoscale

ARTICLE

Supporting Information

Study of the role of iron nitrides embedded in N-doped amorphous carbon as highly active catalyst toward oxygen reduction reaction

Min Wang, [†] *Yushi Yang,* [†] *Xiaobo Liu,* [†] *Zonghua Pu,* [†] *Zongkui Kou,* [†] *Peipei Zhu,* [†] *and Shichun Mu**[†]

[†]State Key Laboratory of Advanced Technology for Materials Synthesis and Processing, Wuhan University of Technology, Wuhan 430070, China

Corresponding e-mail Address: E-mail: msc@whut.edu.cn

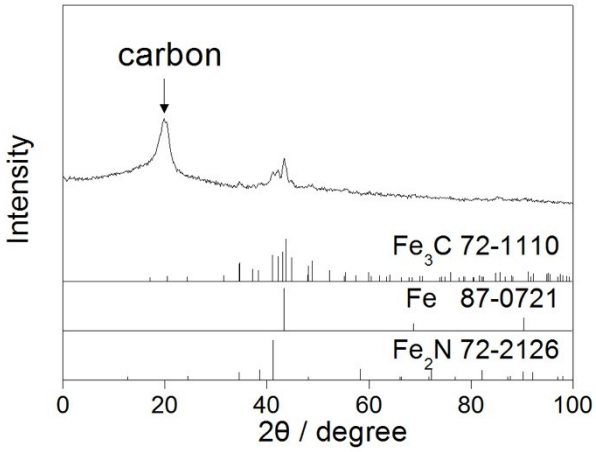

Figure S1. XRD pattern of FeGH-ArNH_3-L

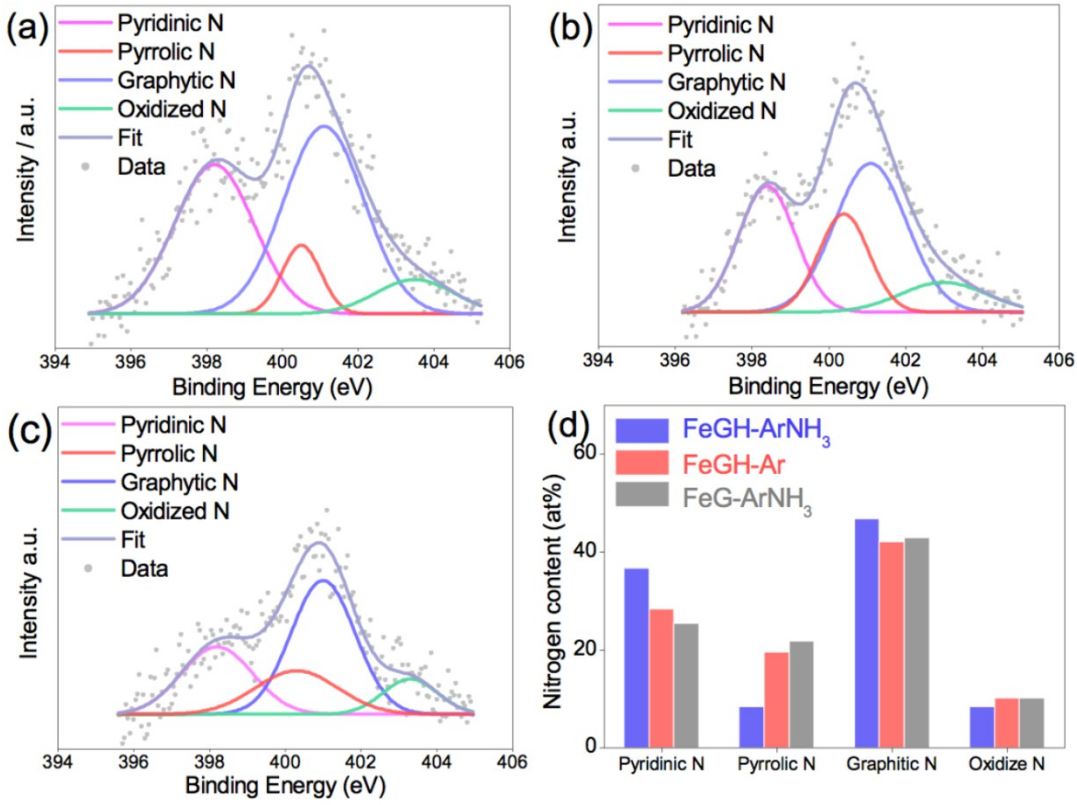

Figure S2. High-resolution N 1s spectra of (a) FeGH-ArNH_3, (b) FeGH-Ar, (c) FeG-ArNH_3, and (d) the relative contents of each N in three samples.

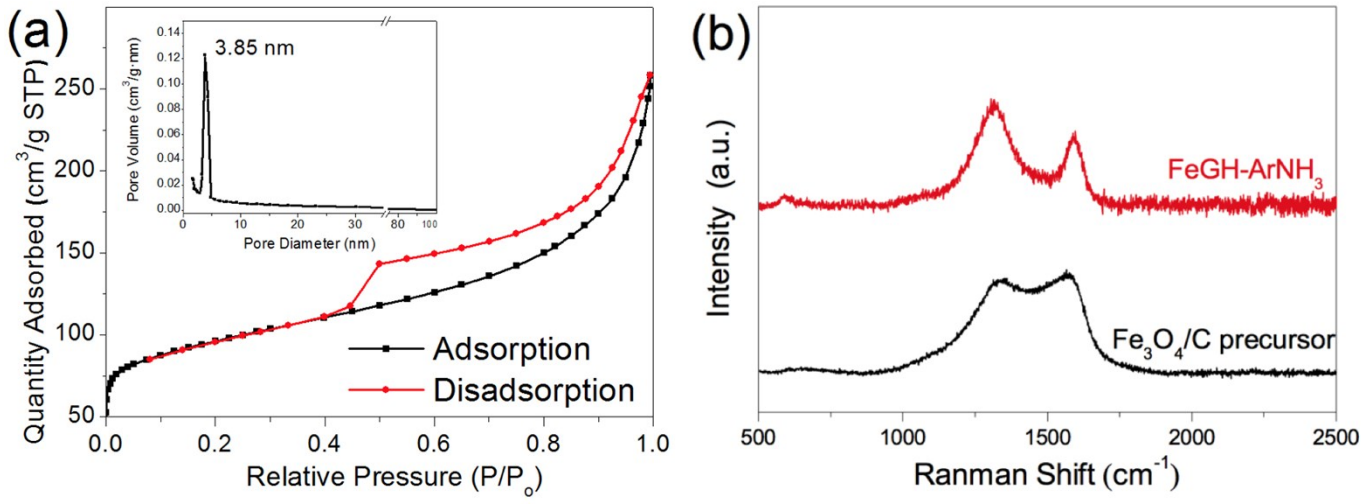

Figure S3. (a) N_2 adsorption/ desorption isotherm of FeGH-$ArNH_3$ (inset: pore size distribution of FeGH-$ArNH_3$). (b) Raman spectroscopy of the Fe_3O_4/C precursor and FeGH-$ArNH_3$.

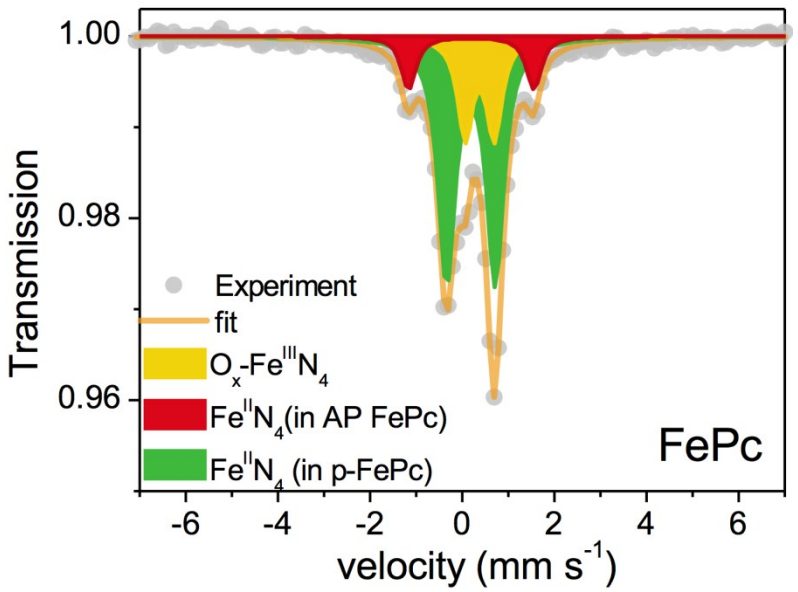

Figure S4. ^{57}Fe Mössbauer spectra of FePc.

Table S1. Table of fitted Mössbauer parameters and the corresponding assignment to each species of FeGH-$ArNH_3$ and FeG-$ArNH_3$. The isomer shift (IS), quadrupole splitting (QS), hyperfine field (H) and the relative absorption area of each species (Area) are given.

		Assignment	IS (mm/s)	QS(mm/s)	H (KOe)	Area (%)
FeGH-$ArNH_3$	Doublet 1	ε-$Fe_{2+x}N$ (x≤0.1)	0.270(15)[(a)]	0.468(42)	-	63.3(28)
	Doublet 2	ζ-Fe_2N	0.431(12)	0.249(17)	-	7.9(21)
	Sextet 1	α-Fe	0	0	332.7(54)	4.0(14)
	Sextet 2	Fe_3C	0.210(47)	-0.030(41)	205.4(30)	24.8(31)
FeG-$ArNH_3$	Doublet 1	ε-$Fe_{2+x}N$ (x≤0.1)	0.317(34)	0.459(87)	-	37(12)
	Doublet 2	ζ-Fe_2N	0.418(14)	0.250(19)	-	47(13)
	Sextet 1	Fe_3C	0.214(84)	0.017(77)	207.2(54)	15.9(43)
FePc	Doublet 1	O_x-Fe^{III}-N_4 [1,2]	0.188(27)	1.063(57)	-	64.2(65)
	Doublet 2	Fe^{II}-N_4 (in amorphous FePc) [3,4,5]	0.380(64)	0.70(13)	-	23.4(56)
	Doublet 3	Fe^{II}-N_4 (in p-FePc) [5,6]	0.194(22)	2.709(45)	-	12.4(19)

(a) Errors are given between parenthesis.

Table S2. Iron contents (molar ratios) toward each phase of FeGH-$ArNH_3$ and FeG-$ArNH_3$ based on the results of their Rietveld refinement showed in Figure 2.

	FeGH-$ArNH_3$	FeG-$ArNH_3$
ε-$Fe_{2+x}N$	45.5%	16.7%
ζ-Fe_2N	20.2%	62.7%
Fe	13.5%	4.6%
Fe_3C	20.7%	8.0%
Fe_4N	0.0%	8% (2% Fe I and 6% Fe II)(*)

(*) the cubic Fe_4N should have two sextets in Mössbauer spectrum due to its two kind of iron sites: 1) those at corner position (Fe I) which in neutral state; 2) those occupying the face-center position (Fe II) with two neighboring N atoms.[7,8]

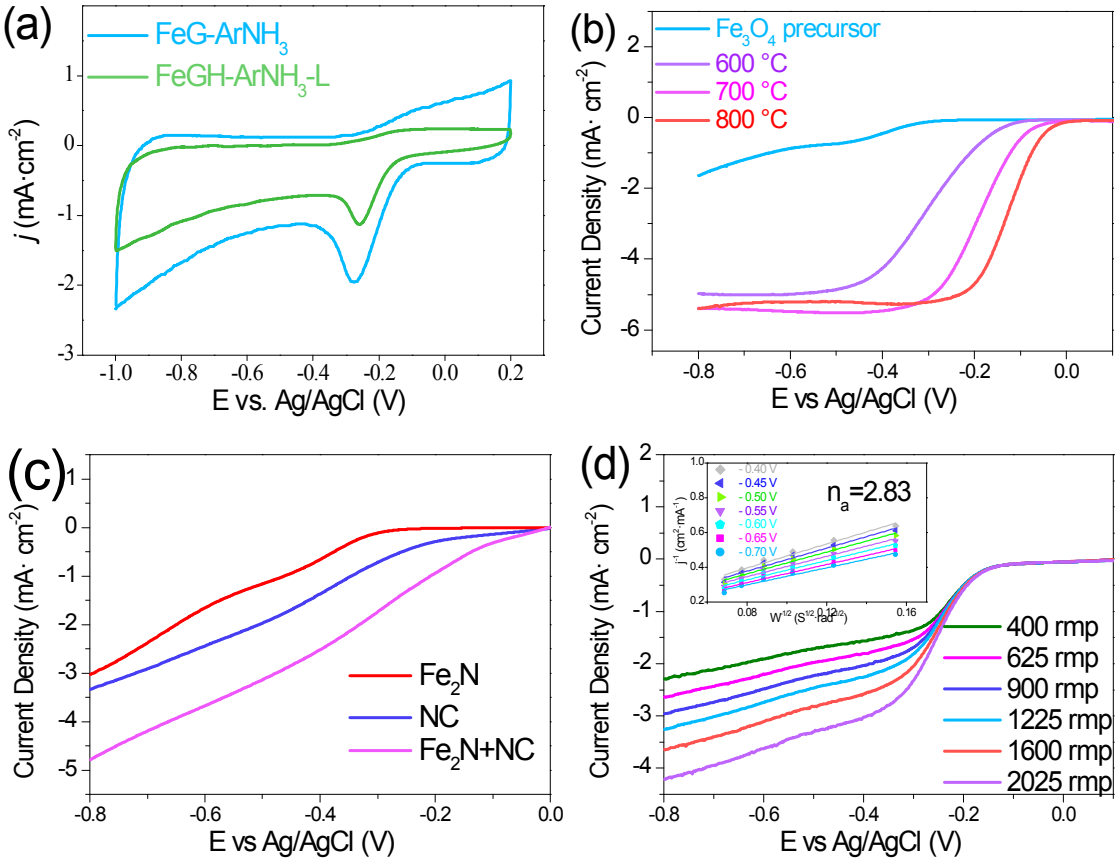

Figure S5. a) CV curves of FeG-$ArNH_3$ and FeGH-$ArNH_3$-L in O_2-saturated 0.1 M KOH solution. b) LSV curves of Fe_3O_4/C precursor and the catalysts pyrolyzed at different temperatures, c) LSV curves Fe_2N, NC and physical mixture of Fe_2N and NC in O_2-saturated 0.1 M KOH solution at 1600 rpm, d) LSV curves of FeGH-$ArNH_3$-L at various rotation rates in O_2-saturated 0.1 M KOH solution; the inset is the corresponding K-L plots at different potentials.

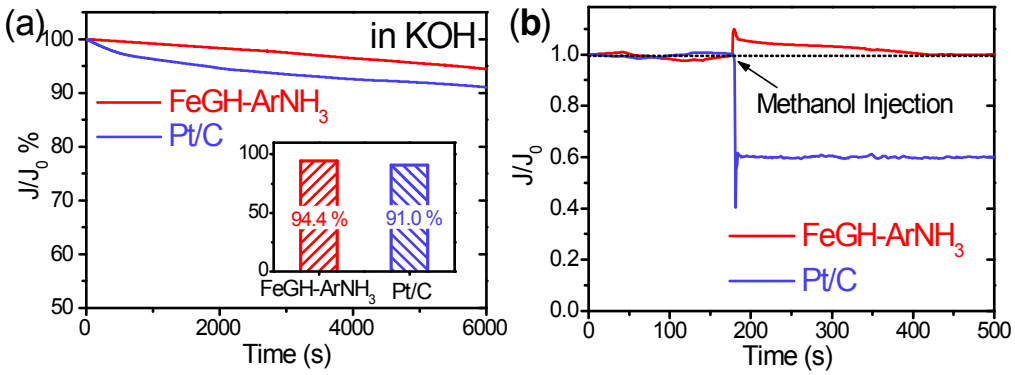

Figure S6. Chronoamperometric (i-t) response of FeGH-$ArNH_3$ and Pt/C at – 0.4 V vs. Ag/AgCl in O_2-saturated aqueous solution of **a)** 0.1 M KOH. (The inset is the retained ratio of the current density of FeGH-$ArNH_3$ and Pt/C). **b)** 0.1 M KOH + 1 M methanol.

Rietveld Refinement

The refinements were performed with assistance of software GSASII.[9] The phase composition, background function, sample displacement, lattice constant and crystallite size were allowed to change during the refinement. The peak width function is obtained from the standard silicon (NIST 640e). For both FeG-$ArNH_3$ and FeGH-$ArNH_3$, their starting phase compositions were from the quantitative analysis of the Mössbauer spectroscopy, which is exhibited later in this paper.

DFT Calculation

The valence electrons were described by plane-wave basis sets with the cutoff energy of 380 eV. All the slabs were separated by a vacuum of 14 Å along the vertical direction to avoid the interaction. The top one layer of each slab was relaxed during the geometry optimization and other layers were kept fixed.[10] For (100), (110) and (111) surfaces of ε-Fe_2N, the Brillouin zone was sampled using Monkhorst-pack[11] (5 × 5 × 1), (5 × 5 × 1), (6 × 6 × 1) k-points, respectively. For (100), (110) and (111) surfaces of ζ-Fe_2N, the the Brillouin zone was sampled at (5 × 5 × 2), (5 × 5 × 1), (4 × 4 × 1) k-points. The atoms were fully relaxed

using the Broyden-Fletcher-Goldfarb-Shanno (BFGS) scheme until the maximum force on them was less than 0.01 eV/Å. The results had been checked for convergence about the cutoff energy and k-points.

Reference

(1) Li, J.; Ghoshal, S.; Liang, W.; Sougrati, M.; Jaouen, F.; Halevi, B.; McKinney, S.; McCool, G.; Ma, C.; Yuan, X.; Ma, Z.-F.; Mukerjee, S.; Jia, Q. *Energy Environ. Sci.* **2016**, *9* (7), 2418–2432.

(2) D. A., S.; C. A., F.; D., T.; L. S., G.; E. B., Y. *J. Electroanal. Chem.* **1984**, *4* (184), 419–426.

(3) Kramm, U. I.; Herrmann-geppert, I.; Behrends, J.; Lips, K.; Fiechter, S.; Bogdanoff, P. *J. Am. Chem. Soc.* **2015**, *138* (2), 635–640.

(4) Sa, Y. J.; Seo, D.; Woo, J.; Lim, J. T.; Cheon, J. Y.; Yang, S. Y.; Kim, C. S.; Kim, M. G.; Kim, T.; Joo, S. H. *J. Am. Chem. Soc.* **2016**, 138, 15046–15056.

(5) Tanaka, A.; Fierro, C.; Scherson, D.; Yeager, E. B. *J. Phys. Chem.* **1987**, 91, 3799–3807.

(6) Blomquist, J.; Moberg, L. C.; Johansson, L. Y.; Larsson, R. *Inorganica Chim. Acta* **1981**, 53, 39–41

(7) Bainbridge, J.; Channing, D. A.; Whitlow, W. H.; Pendlebury, R. E. *J. Phys. Chem. Solids* **1973**, *34*, 1579–1586.

(8) Zhou, W.; Qu, L. J.; Zhang, Q. M.; Wang, D. S. *Phys. Rev. B* **1989**, *40*, 6393–6397.

(9) Toby, B.H.; Von Dreele, R.B. *J. Appl. Crystallogr.* **2013**, 46, 544–549.

(10) Pfrommer, B. G.; Cote, M.; Louie, S. G.; Cohen, M. L. *J. Comput. Phys.* **1997**, *131*, 233–240.

(11) Monkhorst, H. J.; Pack, J. D. *Phys. Rev. B* **1976**, *13*, 5188－5192.

